A New Approach to Characterise the Impact of Rock Bridges in Stability Analysis

# A New Approach to Characterise the Impact of Rock Bridges in Stability Analysis

Davide Elmo & Beverly Yang

NBK Institute of Mining Engineering, University of British Columbia, Vancouver, Canada

Doug Stead

Department of Earth Sciences, Simon Fraser University, Vancouver, Canada

Gianluca Marcato

CNR, Istituto di Ricerca per la Protezione Idrogeologica, Padua, Italy

Lisa Borgatti

DICAM Dipartimento di Ingegneria Civile, Chimica, Ambientale e dei Materiali, Università di Bologna, Bologna, Italy

## Abstract

Rock bridges have been the subject of considerable research since the 1970's with a focus on developing methods to measure rock bridges and quantifying their role with respect to rock mass strength. In the literature, rock bridges are generally defined as a portion of intact rock separating discontinuity surfaces; however, whether a portion of intact rock resists failure and, therefore, represents a critical rock bridge depends on the failure mechanisms that may develop within the rock mass. The difficulty of defining what constitutes a rock bridge is associated with the challenge of measuring rock bridges in the field. This aspect is often ignored by engineers and practitioners, who fail to recognise that rock bridges could exist even within a rock mass characterised by fully continuous surfaces. Furthermore, field evidence of rock slope failure shows that rock bridges do not fail at the same time, and a simple definition of a rock bridge as the distance between existing discontinuities cannot account for progressive rock

mass damage and changes in stresses within a rock mass. The authors suggest that the concept itself of rock bridges may be flawed, and more attention should be given to better understanding damage-related processes, including time-dependent damage in the context of engineered structures.

# 1 Introduction

Rock bridges have been the subject of considerable research since the 1970's, with a focus on developing methods to measure rock bridges and quantifying their role with respect to rock mass strength (e.g., Terzaghi 1962; Jennings 1970; Call and Nicholas 1978; Einstein et al. 1983; Read and Lye 1984; Baczynski 2000, 2008; Kemeny 2005; Dershowitz et al. 2017; Elmo et al. 2009, 2018; Spreafico et al. 2017; Romer and Ferentinou 2019). Note that all those authors have considered rock bridges in the context of natural and engineered slopes; rock bridges in the context of underground excavations are seldom discussed in the literature.

The difficulty in defining what constitutes a rock bridge is associated with the challenge of observing and measuring rock bridges in the field. In the context of slope stability analysis, Elmo et al. (2018) have categorised rock bridges as: in-plane basal (acting across a discontinuity surface), in-plane lateral release (a specific type of in-plane rock bridge, occurring across typically sub-vertical discontinuity surfaces), and down-slope rock bridges (positive or negative with respect to their dip angle). These definitions are graphically illustrated in Fig. 1. The difference between positive and negative down-slope rock bridge is of extreme importance. The former represents the only type of rock bridges considered in Jennings (1970); however, rock mass failure may often include a component of down-slope negative rock bridge fracture.

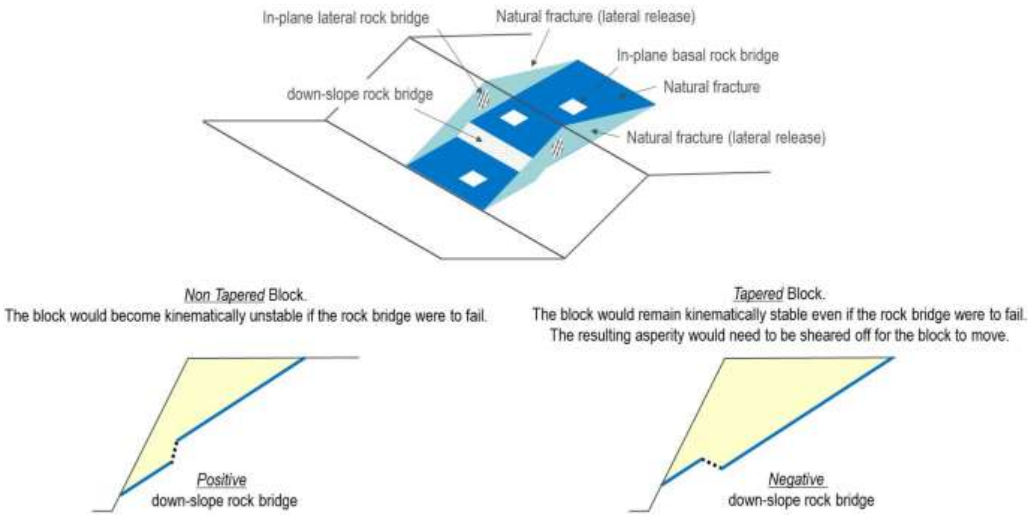


Fig. 1: Illustration showing the definition of rock bridges (Modified from Elmo et al. 2018).

Furthermore, it is important to differentiate between critical and non-critical rock bridges; the former are involved in the generation of failure surfaces or rear/lateral release, while the latter may only be involved in fragmentation of the rock mass during movement. Whether a portion of intact rock resists failure and, therefore, represents a critical rock bridge depends on the failure mechanisms that may develop within the rock mass. In this paper, we present supporting arguments to the claim that rock bridges cannot be truly defined without more attention being given to better understand damage-related processes, including time-dependent damage. In other words, the question is not so much as whether rock bridges actually exist, rather whether their definition is conditional on the specific rock engineering problem, loading conditions and failure mechanism being addressed.

To answer these important questions, this paper will focus on three key objectives:

(i) Using field evidence to demonstrate how rock bridges are not discrete measurable physical features. Rock bridges exist only within the domain of our engineering experience, and they reflect brittle failure mechanisms rather than distinct geological structures.

(ii) Introducing a clear distinction between intact rock bridge problems and rock mass bridge problems. For the latter, understanding the role that damage plays in rock mass bridge failure remains challenging as simulations of discontinuous rock masses are typically carried out by simplifying (truncating) the intensity and size distribution characteristics of the natural fracture network. The result is a form of hybrid equivalent continuum model in which rock mass bridges separates major discontinuities several metres apart from each other.

(iii) Introducing a new rock mass quality indicator, the NCI—network connectivity index, which is capable, when integrated within explicit simulations of rock damage, to address the fundamental question of rock mass strength as a function of the underlying network connectivity. The result is the definition of a rock bridge potential, which, depending on the imposed loading conditions, may be greater than zero even in the case of very blocky and interconnected rock masses.

# 2 Rock Bridges: A Field Perspective

It is not possible to understand the true impact of rock bridges on rock stability without considering field evidence of their existence. In the field, failure of intact rock bridges may reflect the presence of proto joints (e.g., Hencher et al. 2012), sedimentary structures on bedding surfaces, or undulations due to tectonic activity. Furthermore, field evidence of rock slope failure shows that rock bridges do not fail at the same time, and the definition of rock bridges as two-dimensional distances between existing discontinuities is extremely simplistic

and cannot truly account for potential damage accrued due to stress redistribution (Elmo et al. 2018). The following sections present field examples of failure mechanisms associated with the presence of rock bridges. These examples have in common one fundamental aspect of rock engineering design: there is no geological feature to which we can point to and call a rock bridge until the rock bridge has failed. A corollary to that statement is that any intact portion of a rock mass has the potential to be a rock bridge; while seemingly obvious, this statement is ignored in most commonly adopted approaches for rock bridge strength characterisation, which are founded on the concept of step-path failure developing exclusively between a set of non-persistent discontinues.

## 2.1 Field Evidence of Rock Mass Stability due to Intact Rock Bridges

Figures 2 and 3 show how the presence of rock bridges could manifest even within a rock mass characterised by apparently fully continuous and interconnected fractures. Their existence and geometrical definition would be linked to the slope structural characteristics and the induced stress field responsible for the observed rock damage; note that methods commonly used to measure rock bridges (e.g., Jennings 1970; Stacey and Read 2009) that exclusively consider failure pathways by connecting one set of non continuous and down-slope dipping fractures would not be able to replicate the conditions shown in Figs. 2 and 3.

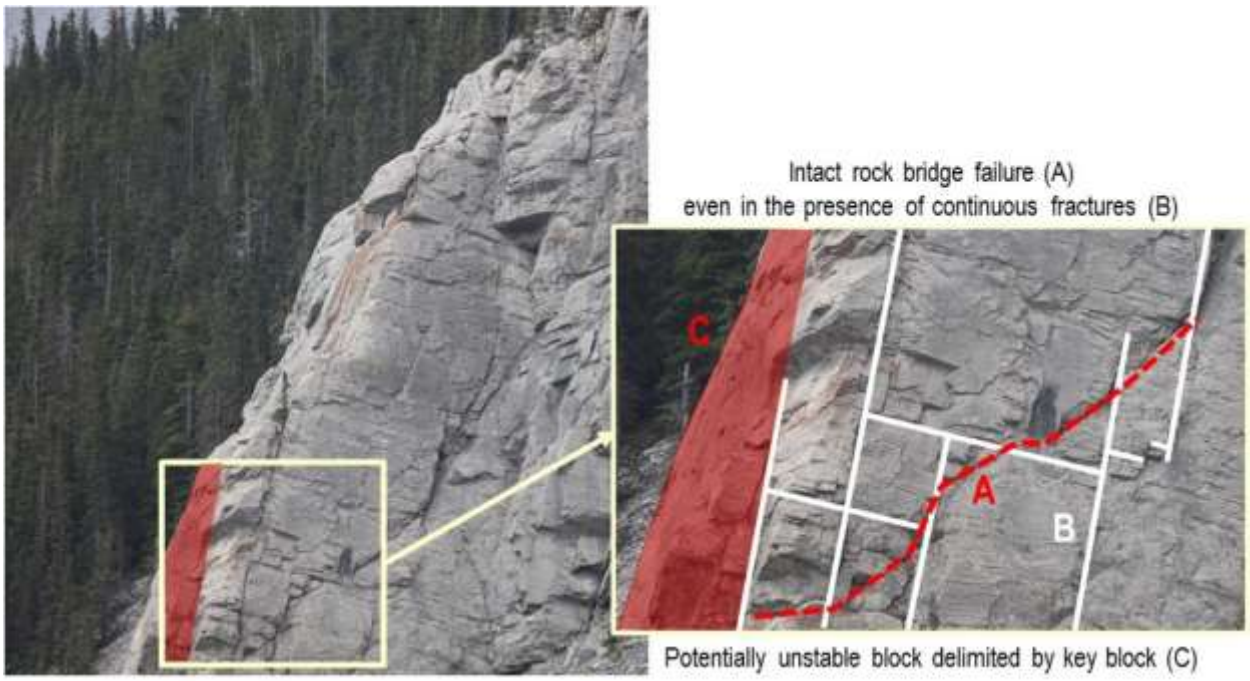


Fig. 2 Example showing how ongoing intact rock bridge failure may occur even in the presence of apparently continuous fractures (Modified from Elmo et al. 2018).

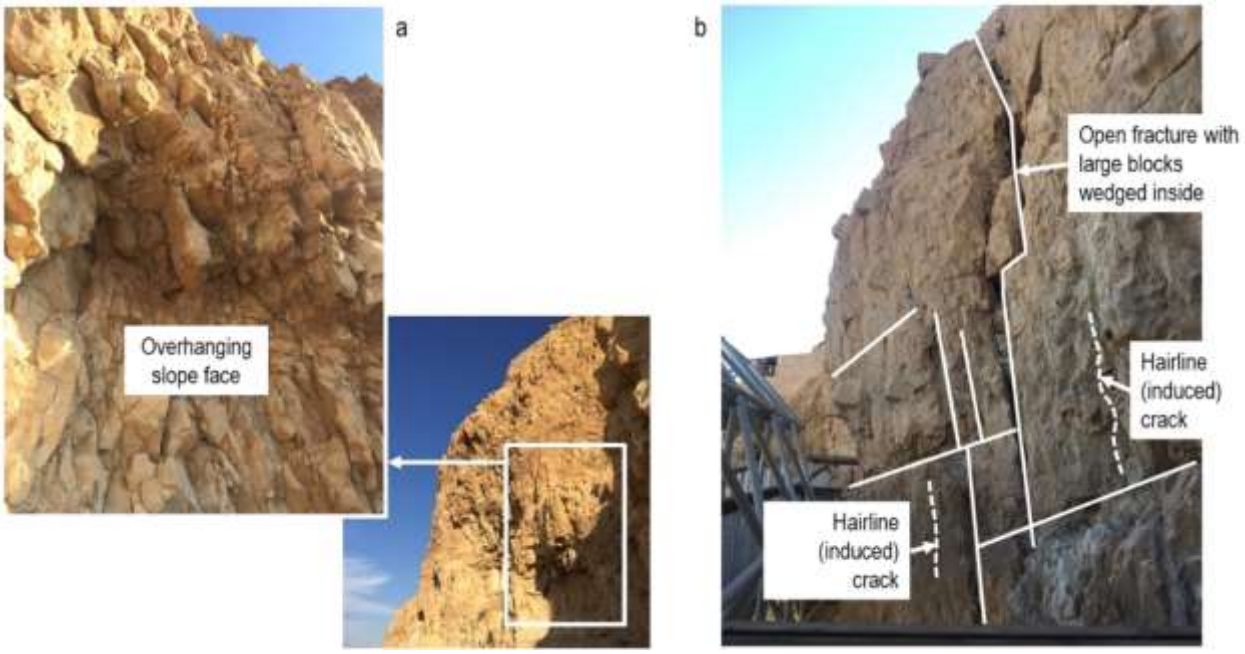


Fig. 3 a) Example of an overhanging rock face with multiple fracture sets resulting in partially formed blocks; and b) further example of how the presence of apparently continuous fractures do not exclude the presence of rock bridges

Both Figs. 2 and 3 describe a typical bias that occurs when analysing and mapping rock exposures, that is, fractures traces are generally projected as continuous 2D structures within the rock mass. Under these circumstances, in-plane rock bridges are generally ignored. Shang et al. (2017) presented an interesting technique called “forensic excavation” for investigating the existence of in-plane rock bridges that clearly revealed how rigorous rock bridge measurements would be possible only after failure has occurred. This is demonstrated by the field example shown in Fig. 4, which depicts a failed block that was once overhanging in a side niche of an abandoned tunnel (Passo della Morte, Italy). Photographic evidence shows that the block remained in place for several years before it failed, at which point it was possible to confirm the extent of the rock bridge that contributed to its stability. Moreover, the Passo della Morte site offers a good example of the role of intact rock damage (rock bridge failure) in the creation of failure surfaces (Fig. 5). For instance, field observations support the notion that trace B1 is not continuous inside the slope. The origin of trace B1 could be due to brittle failure associated with buckling of the limestone beds; however, the resulting failure is limited to a narrow outer section of the slope. A similar mechanism can be observed along traces B2, C1 and C2. Consequently, it is reasonable to assume that the stability of the Passo della Morte rock slope is controlled by inherent tectonic damage rather than by in-plane rock bridges acting across pre-defined failure surfaces.


Fig. 4 Pre- and post-failure images of a rock block whose stability was apparently controlled by the presence of rock bridges

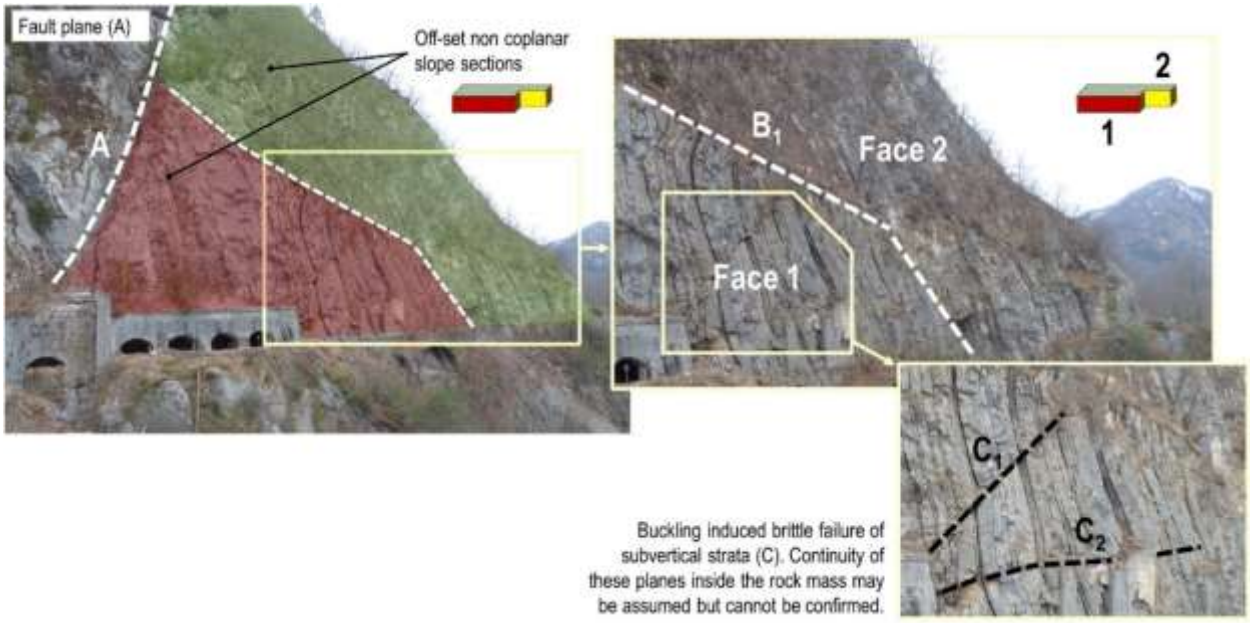


Fig. 5 Field example (Passo della Morte, Italy) showing the role of intact rock damage (rock bridge failure) associated with buckling mechanisms contributing to the creation of failure surfaces (traces B1, B2, C1 and C2)

Figure 6 shows a rock slope failure in British Columbia (near Squamish, British Columbia) that occurred in 2015. Sampaleanu (2017) and Sampaleanu et al. (2017) suggested that failure was caused by root pressure behind a block causing a progressive toppling, which in turn crushed the outer edge of the underlying block, causing failure. Iron staining along the fracture plane denotes possible water infiltration, and thus could be used as an indicator of the persistence of

the fracture surface prior to failure. Root pressure and freeze–thaw cycles can be key factors controlling the failure of rock bridges in natural slopes. However, their role is seldom considered in numerical models, since the impact of rock bridges on the stability of a structure excavated in rock typically focuses on rock bridge strength in relation to excavation-induced stresses.


Fig. 6 Pre- and post-failure photographs of a rockfall failure in Squamish, B.C., Canada (Golder Associates, 2015 in Sampaleanu 2017)

A prior knowledge of the volumes of the quasi-stable blocks shown in Figs. 4 and 6 would not have been sufficient to determine the extent of the rock bridge prior to failure, since their stability was determined by three unknown variables: (i) rock bridge area; (ii) intact rock tensile strength; and (iii) the actual stability condition of the blocks, in other words their factor of safety. More importantly, none of these variables are time invariant. In the example shown in

Fig. 4, it is reasonable to assume that alteration of the intact rock conditions over time caused the rock tensile strength to decrease, which in turn led to progressive damage (i.e., decreasing of the rock bridge area) and eventually failure of the block. In their simplicity, these example demonstrates the importance of considering the time dependency of progressive failure of intact rock bridges (Kemeny 2005) and the impact of weathering on intact rock strength, and tensile strength in particular (Arikan et al. 2007; Alzo'ubi 2009). However, time dependency of intact rock properties is often ignored in analyses of rock bridges (Elmo et al. 2020a, b).

# 3 Rock Bridges as Geotechnical Known Unknowns

The discussion above appears to identify a major problem for design scenarios, since in the absence of visible failed surfaces, rock bridges become a matter of known unknowns. A back analysis of an existing—but not yet failed—rock slope to determine the key role that rock bridges play in their stability may not necessarily lead to conclusive results, due to the impossibility of precisely determining the current stability state of the rock slope (i.e., its corresponding factor of safety) and the impossibility of determining the precise location of the rock bridges and their strength. Even if the numerical analysis was to be calibrated against monitoring data, the uncertainty would remain as to whether the assumptions made in the analysis with respect to size and location of the rock bridges are correct. There may be instances in which remote sensing techniques (e.g., thermal imaging) may be able to detect rock bridges prior to failure (Guerin et al. 2019). Although very promising, the approach appears to be limited to the case of cliff-parallel exfoliation fractures and partially detached exfoliation sheets.

When describing the role that rock bridges play in the stability of both surface and underground excavations in rock, one may argue that the existence and definition of rock bridges represents a form of phenomenal evidence, that is evidence obtained by human perception, rather than objective—factive—evidence (Schellenberg 2016). Despite both phenomenal and factive evidence employing our capacity to perceive, factive evidence is supported by objective and measurable data, while phenomenal evidence is only supported by our experience and engineering judgment, which are impacted by cognitive biases and therefore can be flawed (Elmo and Stead 2020). In rock engineering, phenomenal evidence is exacerbated by what in physics has been termed the "observer effect", according to which the observation and measurement of a phenomenon (e.g., rock bridges) is associated with a change in the phenomenon being measured, in this case the failure of the rock mass exposing the surfaces along which the rock bridges were acting (Elmo et al. 2018). Because (as shown earlier in Figs. 2, 3, 4, 5, 6) critical rock bridges exist in relation to their potential to resist failure, intact rock damage in between natural discontinuities would represent a potential sign for the occurrence

of rock bridges, but it would not be evidence of whether they would be important in slope stability. Because of their known unknown nature, rock bridges cannot be incorporated in design analysis as deterministic features and we should look at rock bridges in the context of risk analysis, whereby both the probability of occurrence of rock bridge and the consequence of their failure are described by a range of scenarios.

Indeed, the definition of rock bridge generally encountered in the literature does not account for “block forming potential”, “block kinematics” conditions, scale effects, and it ignores the case in which a rock bridge may exist and fail despite fractures forming a continuous pathway (Elmo et al. 2018). Furthermore, rock bridge problems are directionally dependent: a rock bridge could exist in one direction but not be present in other directions.

Even if one accepts the validity of the 2D classical approach to rock bridges, rock bridge problems should not ignore the kinematic characteristics of the resulting rock mass wedge and relevant aspects of block theory (Elmo et al. 2018). Using the approach of Jennings (1970), a bias is introduced when measuring so-called rock bridge percentages if a condition is imposed which neglects cases in which failure of intact rock bridges would result in a negative stepped failure path and the formation of a tapered rock mass wedge. Accordingly, 2D rock bridge strength characterisation typically ignores negative down-slope rock bridges (as defined earlier in Fig. 1) based on the argument that their presence would increase rock mass stability by eliminating the kinematic freedom of the resulting block. This assumption, however, is not necessarily true. While in purely geometrical terms, negative down-slope rock bridges may contribute to increase shear resistance, they would also lead to stresses being redistributed within the rock mass creating the potential for intact rock damage (e.g., Fig. 2). For example, a negative down-slope rock bridge near the toe of a rock slope may fail if sufficient intact rock damage occurs resulting in an alternative failure path by-passing the negative rock bridge itself (Fig. 7a). Similarly, a negative down-slope rock bridge could also increase the kinematic potential for block failure in the case of an active–passive block mechanism where the negative rock bridge contributes to rock mass dilation (Fig. 7b). In other words, negative rock bridges may both favour interlocking and at the same time cause stress redistribution and both intra- and inter-block intact rock damage.

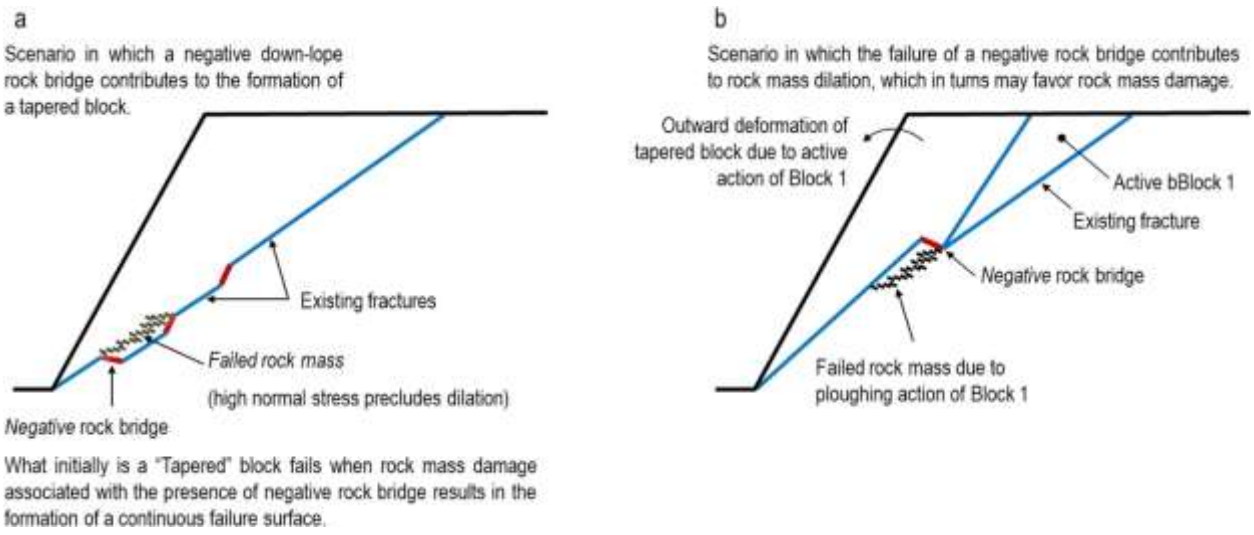


Fig. 7 a) Impact of negative down-slope rock bridges. B) Failure due to stress redistribution and resulting rock mass damage; and c active–passive wedge mechanisms (Adapted from Elmo et al. 2018).

# 4 Modelling Simplification: Intact Rock Bridges vs. Rock Mass Rock Bridges

When employing numerical analysis to simulate a naturally fractured rock mass and the associated rock bridges, it is not computationally feasible to explicitly include natural discontinuities at a scale ranging from cm length to metre, and tens of metres length. The adopted upscaling process (i.e., removal of relatively shorter fractures) produces models in which intact rock bridges (mm- to cm- scale) are substituted by equivalent continuum rock mass bridges (metre scale) (Fig. 8). In principle, every rock mass bridge could be treated as an independent synthetic rock mass bridge (SRMB) model. However, the issue still arises as to whether it would be correct to apply the same loading conditions to all SRMB models.

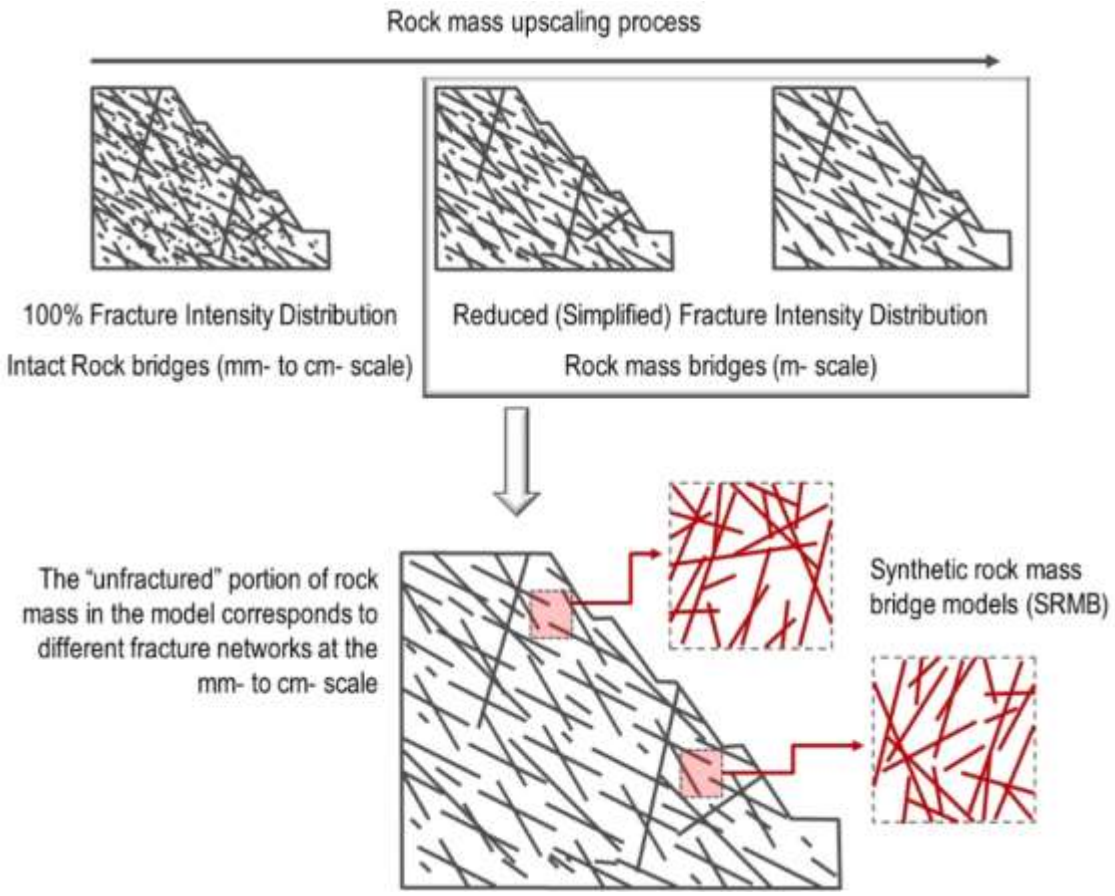


Fig. 8 Definition of an intact rock bridge and a rock mass bridge as a function of the upscaling process

For a rock slope scenario as depicted in Fig. 8, loading conditions would be spatially variable; and we would need to consider that loading conditions for different SRMB models would change interdependently as progressive damage accrues in the slope. This aspect highlights one of the major limitations of statistical analysis of rock bridge failure (both intact and rock mass bridges), that is the imposition of a constant stress field and the lack of consideration of progressive damage. The extent of the damage zone that would develop in every SRMB models would be a function of the variability of the existing fabric (mm- to cm- scale), which in turn corresponds to a different network connectivity.

In the literature (Jennings 1970; Einstein et al. 1983; Baczynski 2000, 2008; Dershowitz et al. 2017; Stacey and Read 2009; Elmo et al. 2009), the strength of rock bridges is generally defined with respect to a rock bridge percentage factor, calculated as the ratio of total length of rock bridges to total length of an equivalent fracture length. The authors believe that the use of rock bridge percentage as indicator of rock bridge strength is misleading, since it represents an

average rock bridge length (or area); the same rock bridge percentage may correspond to a different number of rock bridges, each one of different size; the specific location of the rock bridges is also not accounted for, though it influences the stress magnitude developing across each rock bridge. More importantly, the generally accepted formulations used to calculate rock bridge strength ignore scale effects (Elmo et al. 2018). The authors argue that for rock mass bridge problems, scale effects must be accounted for, since it is well known that rock mass strength decreases with increasing sample size. However, a consideration of scale effect alone is not sufficient, since the strength of a rock mass bridge, would depend on the loading conditions applied to the SRMB models. Due to different imposed normal stress conditions, for the same rock mass fabric and connectivity, the failure mechanism and associated strength will change depending on whether the rock mass bridge is located close to the toe or the crest of the slope. This is shown in Fig. 9 using the results for two SRMB models that will be discussed in Sect. 5.1.1.

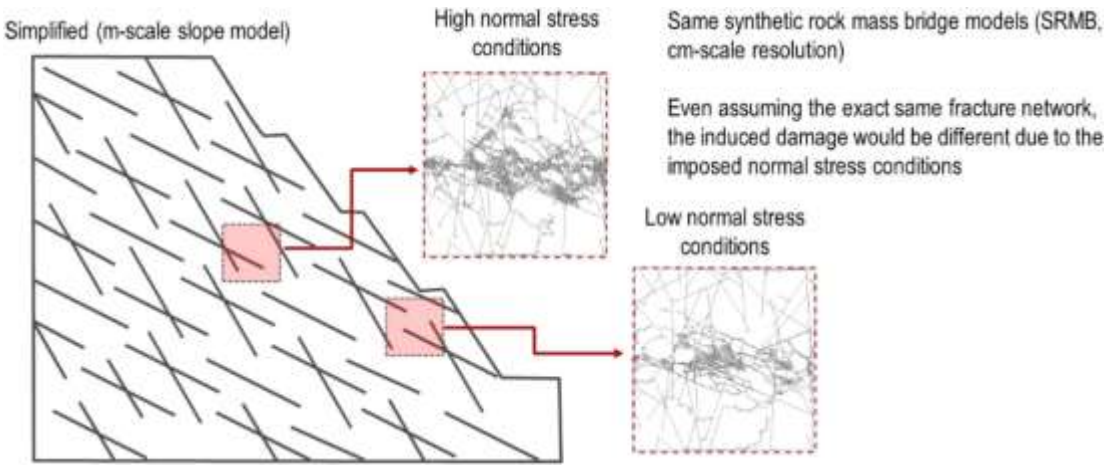


Fig. 9 Example of how progressive rock mass damage would change depending on the location of the rock mass bridge and the imposed normal stress conditions

# 5 Rock Bridge Behaviour: Interdependence of Fracture Connectivity, Stress Field and Material Properties

The previous discussion clearly indicates that the notions of rock bridges and rock bridge strength are rather complex, and rendered even more problematic by the fact that rock bridges cannot be considered an intrinsic and measurable rock mass property. We can postulate the existence of rock bridges, but we cannot confirm nor effectively and routinely measure their dimensions. Accordingly, the authors believe that rock bridge strength should be defined with respect to a novel concept of rock bridge potential that better reflects the interdependence of

key parameters, such as fracture network connectivity, stress field and rock material properties, and better reflects the conditional existence of rock bridges.

The following sections discuss the development of such a rock bridge potential based on the network connectivity index (NCI) parameter introduced by Elmo et al. (2020b).

## 5.1 Network Connectivity Index and Rock Bridge Potential

Several studies have demonstrated that discrete fracture network (DFN) models are effective tools for the characterisation of rock masses (Elmo et al. 2014; Wang et al. 2017). Amongst other, Elmo et al. (2009) and Dershowitz et al. (2017) presented examples of DFN models applied to the study of rock bridges, by identifying potential failure pathways through DFN models. DFN models can also be embedded within geomechanical models to provide a quantitative measurement of rock mass strength directly linked to the structural character of the rock mass (e.g., Elmo and Stead 2010). This is the rationale of the so-called synthetic rock mass (SRM) modelling approach (e.g., Pierce et al. 2007; Elmo et al. 2016). Elmo et al. (2020b) have used the SRM approach has been used to develop a new rock mass classification system that combines fracture intensity, fracture density and fracture intersection density parameters. The approach combines DFN analysis and rock mass classification systems by making the DFN model the source of the input parameters for the classification process.

Any geometrical definition of rock bridges would need to consider the measurement of fracture length (1D), fracture surface area (2D). In the early stage of a project, fracture surface area is generally not available, or has to be inferred based on scaling law relationships. A knowledge of fracture length or fracture surface area is also insufficient, since the existence of rock bridges depends on another important parameter that controls network connectivity, that is, fracture termination, which cannot be measured using 1D data (core logging). Of interest, the ISRM suggested methods for the quantitative description of discontinuities in rock masses (ISRM 1981) lists ten parameters generally recorded when sampling discontinuities in situ. However, no mention is made of fracture terminations as a required parameter to describe discontinuities and rock masses. Not surprisingly, in the literature, the rock bridge problem generally considers intact portions of rock in between pre-existing fractures and thus completely ignore the connectivity of the fracture network.

The importance of network connectivity is well known in the DFN community. For instance, Xu et al. (2006) and Alghalandis et al. (2015) presented a connectivity index in relation to connectivity maps and studied the relationship between the average number of intersections per fracture and the average fracture length per unit area (P21). Alghalandis and Elmo (2018) proposed the use of a DFN approach to study rock bridges with respect to the degree of interlocking of the rock mass. Using RB21 measurements (rock bridge length per unit area, Elmo

et al. 2018) along multiple possible paths in multiple directions they proposed a structural quality index (0–100) such that the higher the rock mass degree of natural fracturing and interlocking, the lower the number of rock bridges available.

The NCI system developed by Elmo et al. (2020b) combines P21, number of fracture intersections per area (I20) and number of fractures per area (P20) using a parameter (NCI) that can be easily measured from sampling of 2D rock exposures or derived from 3D DFN models. In principle, NCI ratings could also be defined with respect to the trace maps that natural fractures produce along the cylindrical surface of a rock core. Compared to other classification systems, the NCI provides a quantitative indicator of rock mass blockiness in relation to the network connectivity, defined as:

$$NCI = \frac{P_{21}}{P_{20}} I_{20} \qquad (1)$$

where P21, P20 and I20 are the areal fracture intensity, the areal fracture density and areal fracture intersection density, respectively. The parameter I20 in the NCI formulation is corrected to account for censoring effects and shape effects (i.e., width-to-height ratio of the mapping window relative to loading direction). For a given SRMB or mapped window, Xt, Xr, Xl, Xb and Xint are the number of intersections on the top, right, left, bottom and internal intersections, respectively (Fig. 10).

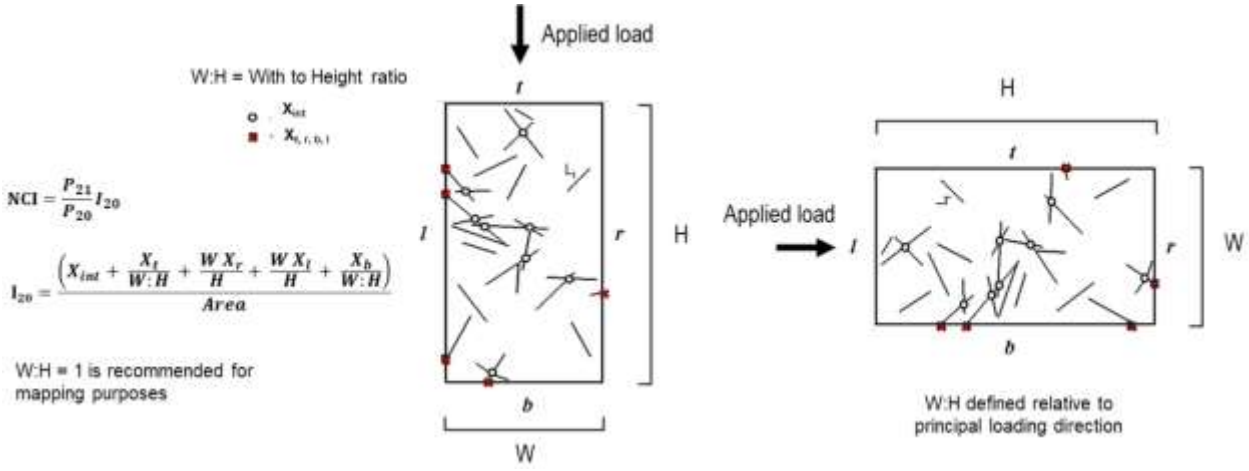


Fig. 10 Definitions of internal and boundary intersections for a rock mass window with dimensions W (width) and H (height)

The basic principle of the NCI approach is that the longer the average fracture trace length and the greater the number of fracture intersections, the blockier the rock mass. A relatively low NCI rating implies that rock bridge failure occurs by connecting existing fractures (positive and/or negative rock bridges), while for a high NCI rating rock bridge failure may predominantly

be in the form of intra-block damage. The NCI approach allows one to determine whether rock mass behaviour is related to the characteristics of the fracture network, or if rock mass behaviour is largely a stress-driven damage accumulation process (e.g., spalling), or a combination of stress-driven failure and sliding along existing fractures. Rock masses are inherently variable, and therefore we cannot and should not expect a precise correlation between NCI (or any other rock mass classification rating) and rock mass behaviour, defined by rock mass strength and deformability.

Scale and size effects are often ignored during the classification process, and there is a tendency to consider rock mass classification systems as absolute rather than relative to the size and scale of the problem. Using pillar strength formulae as an analogy, rock mass classification systems are generally formulated based on a shape-effect approach, and the conventional wisdom is that a given geotechnical unit will have a constant rating associated to it independent of changes in its size and shape. However, synthetic rock mass models can directly account for scale and size effects. This is demonstrated in Fig. 11, in which finite-difference element (FDEM) modelling results sourced from Elmo (2006) and Elmo et al. (2020b) are used to plot rock mass strength vs. NCI ratings. The results show that very similar NCI ratings may be associated with a different rock mass response. The same conclusion could be extended to current rock mass classification systems; therefore, it would be incorrect to conclude that two rock masses (same rock type) with the same assigned rating would behave the same under similar loading conditions.

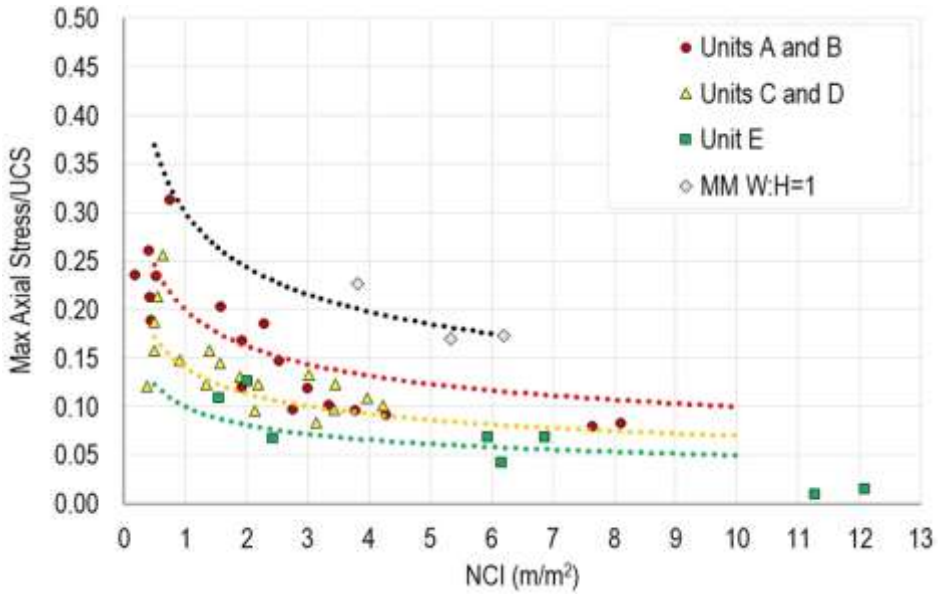


Fig. 11 Plot and preliminary correlation of rock mass strength vs. NCI for two different mine locations, units A–E, and unit MM, respectively

The variability of rock mass strength would decrease for isotropic rock masses at a scale approaching the representative elementary volume (REV). This has been demonstrated in Elmo et al. (2009) using an anisotropy index calculated from the relationship between the strength of hard rock pillars and their initial P21. Note that the anisotropy index would change depending on the shape (width-to-height ratio) of the rock mass being considered, hence the need to correct the parameter I20 in the NCI formulation above.

Using equivalent GSI (geological strength index, Hoek et al. 1995) and conditions of fracture surfaces estimated for the rock masses corresponding to the models shown in Fig. 11, a table has been developed (Fig. 12) that combines GSI ratings and NCI. Note that NCI ranges for massive to blocky, to very blocky are fixed, while the same GSI rating in principle may be assigned to both a massive and a very blocky rock mass depending on the estimated conditions of the fracture surfaces. In this context, NCI helps to better constrain the assumed blockiness conditions when estimating GSI.

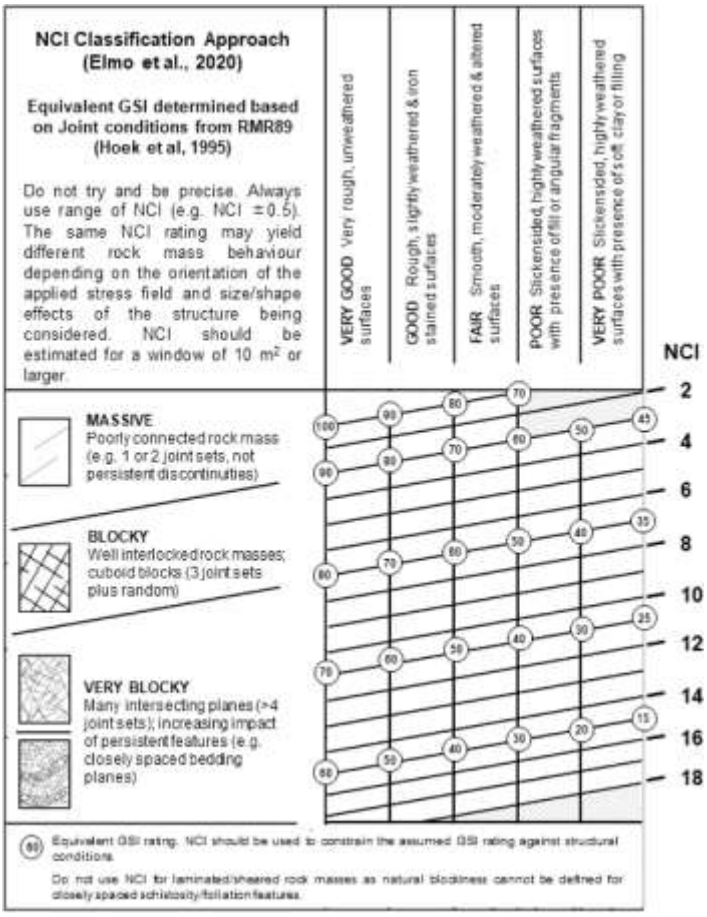


Fig. 12 Preliminary NCI chart based on the GSI by Hoek et al. (1995). NCI should be estimated for a window of 10 m2 or larger

Because new fractures are generated and existing fractures propagate as the rock mass is loaded, the NCI concept could be extended to consider the impact of stress-driven fractures. A stress-driven damage NCI is, therefore, introduced, NCId, where the suffix (d) refers to the damaged state of the rock mass under loading. NCId includes both natural and induced fractures; similarly, NCIrb is the NCI calculated with reference to just the induced fractures. NCId and the rock bridge potential are expressed, respectively, as

$$NCI_d = NCI + NCI_{rb} \quad (2)$$

$$\text{Rock bridge potential} = \frac{NCI_{rb}}{NCI_d} = \frac{NCI_{rb}}{NCI + NCI_{rb}} \quad (3)$$

The ratio between NCIrb and NCId represents the rock bridge potential: the higher the ratio, the higher the contribution of intact rock failure to the overall rock mass behaviour. Figure 13 shows that the relationship between the initial NCI, NCIrb and NCId yields a 3D surface whose slope increases for decreasing NCI and increasing NCIrb. Rock masses with an equivalent NCI may yield a different rock bridge potential based on the degree of fracturing that would result when the rock mass is subjected to loading.

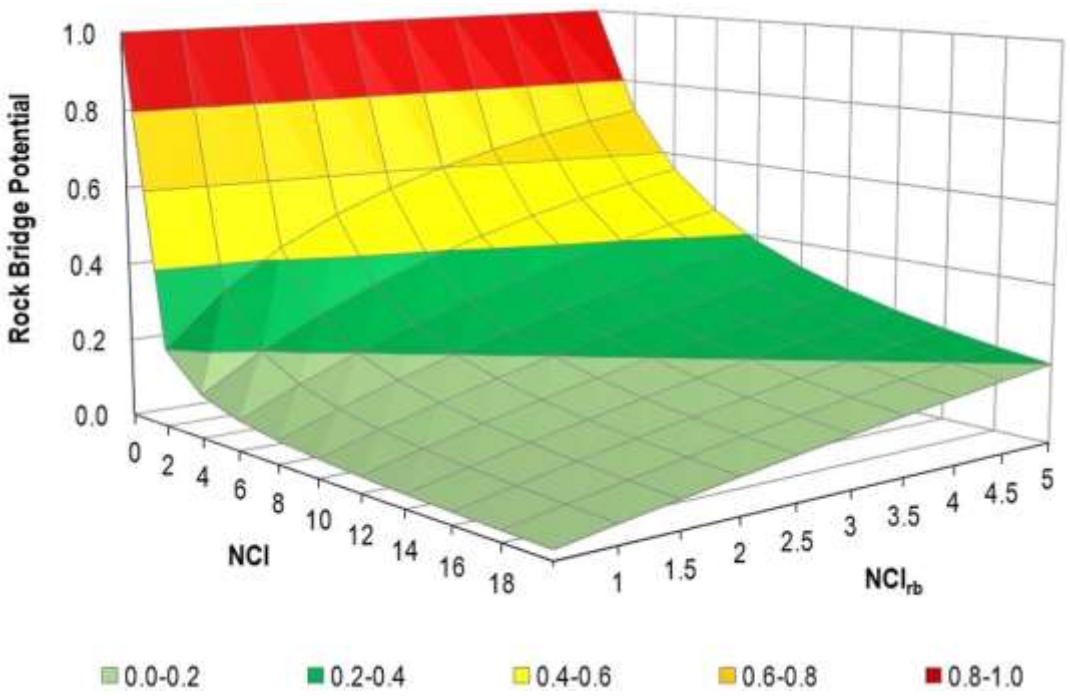


Fig. 13 Definition of rock bridge potential as a function of the initial NCI and the induced NCIrb

### 5.1.1 Modelling Results

SRMB models (15 m scale) using an FDEM approach were used to test the concept of the rock bridge potential presented in the previous section. The FDEM code used in the analysis is the proprietary software Elfen (Rockfield 2019). The FDEM approach (Munjiza et al. 1995; Owen et al. 2004) is well suited for the characterisation and analysis of rock bridges, since it allows the simulation of brittle failure mechanisms, hence the creation of discrete blocks and failure kinematics are fully accounted for.

The analysis combines four models presented in Elmo et al. (2020a) with five new models from the same (undisclosed) mine location. Material properties used in the models are presented in Table 1. Loading conditions are shown in Fig. 14; every SRMB included three different scenarios with normal stress of 0, 2 MPa and 4 MPa, respectively. Because of its proof-of-concept nature, in the currently analysis the NCId and rock bridge calculations have been limited to the modelling scenarios with 0 MPa applied normal stress. Notwithstanding, a rock bridge potential could be calculated for the different normal stress conditions that would be encountered within a rock slope. An automated detection algorithm to provide faster measurements of NCId is being developed to work in combination with different FDEM codes.

Table 1 Material properties used in the FDEM models showed in Fig. 14

| **Intact rock properties** | | **Joint properties** | |
|---|---|---|---|
| Tensile strength (MPa) | 7.1 | Cohesion (MPa) | 0.1 |
| Cohesion (MPa) | 11 | Friction (°) | 31 |
| Friction (°) | 38 | Normal stiffness (GPa/m) | 5 |
| Fracture energy ($J/m^2$) | 15 | Shear stiffness (GPa/m) | 0.5 |

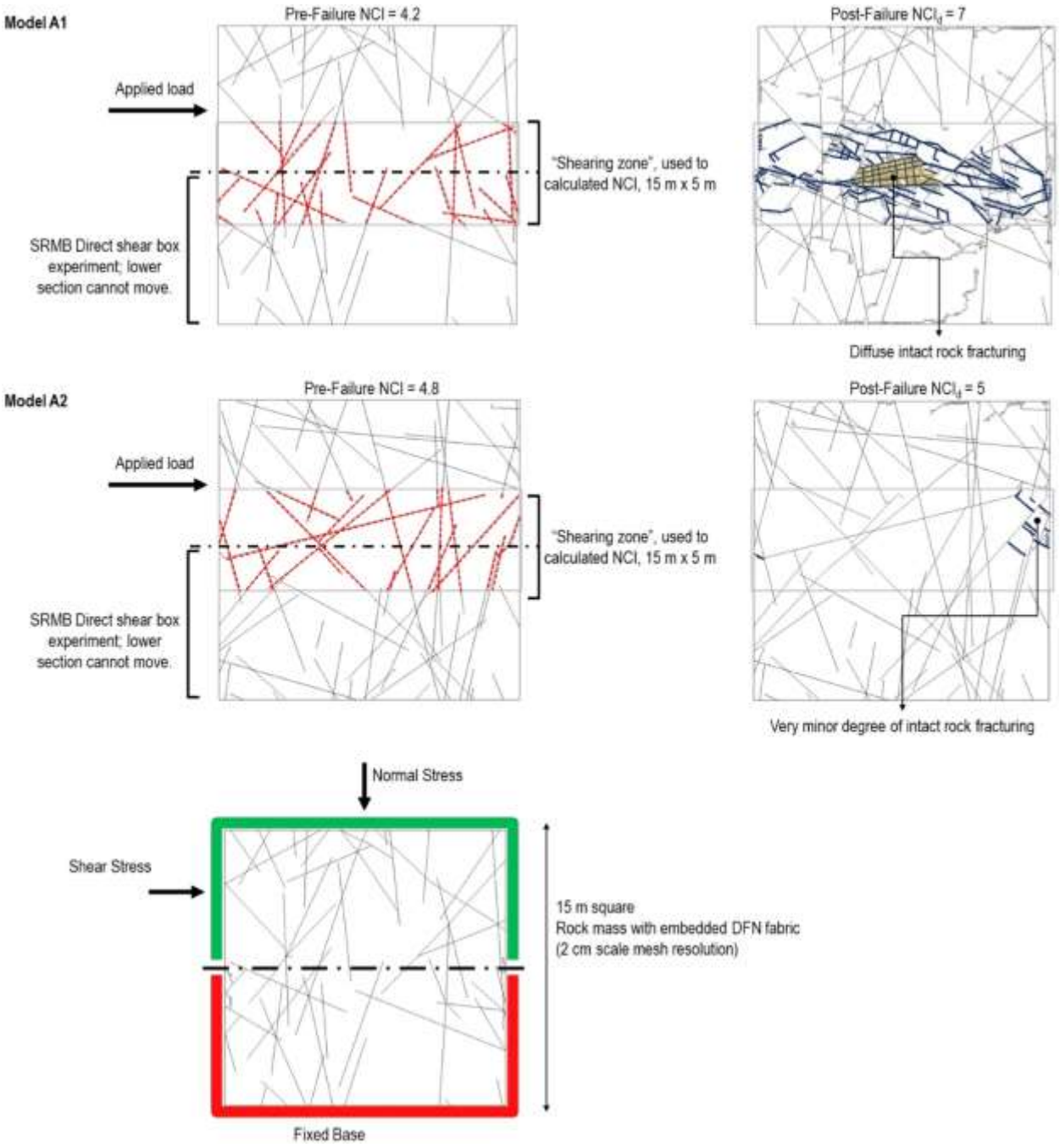


Fig. 14 Analysis of results for Models A1 and A2, pre- and post-failure. Note how a significant degree of intact rock fracturing accompanies the failure of Model A1, despite the two models having comparable initial NCI values. A schematic of the loading conditions (same for all SRMB models) is also provided

The SRMB models replicate a direct shear box experiment, hence the sampling region used to calculate P21, P20 and I20 is assumed to coincide with a sufficiently large area across which

induced fracturing directly contributes to the failure of the simulated rock mass. Furthermore, NCI is calculated considering the horizontal loading conditions; the height (H) of the sample equal 15 m and the width (W) varies as a function of the assumed sampling region (analogous to a slender pillar being axially loaded).

NCIrb values range from 0.06 to 2.8 for models C1 and A1, respectively. Rock bridge potential ranges from 0.01 to 0.6 for models C1 and B1, respectively. In Model C1, failure occurs predominantly by shearing along a relative persistent fracture. Note that a larger rock bridge potential is actually calculated for model B1 (NCI and NCIrb of 1.3 and 2.2, respectively) and not Model A1, which combines a relatively large initial NCI (4.2) and the maximum NCIrb of all the models. The complete set of NCI ratings and rock bridge potentials are summarised in Table 2. Modelling results are presented in Figs. 14, 15, 16 and 17.

Table 2 NCI ratings and rock bridge potentials for all SRMB models shown in Fig. 14

| **Model ID** | **NCI** | **$NCI_{rb}$** | **RBP** | **Modelled rock mass cohesion (MPa)** | **Ratio of modelled cohesion to intact rock cohesion** |
|---|---|---|---|---|---|
| A1 | 4.2 | 2.8 | 0.4 | 2.6 | 0.2 |
| A2 | 4.8 | 0.2 | 0.0 | 0.4 | 0.04 |
| B1 | 1.3 | 2.2 | 0.6 | 4.3 | 0.4 |
| B2 | 4.8 | 0.1 | 0.04 | 0.2 | 0.02 |
| B3 | 3.1 | 0.7 | 0.2 | 1.5 | 0.1 |
| C1 | 6.9 | 0.1 | 0.01 | 0.5 | 0.04 |
| C2 | 4.5 | 1.6 | 0.3 | 2.4 | 0.2 |
| D1 | 1.1 | 1.3 | 0.5 | 3.5 | 0.3 |
| D2 | 3.4 | 0.7 | 0.2 | 1.3 | 0.1 |

1. Note: Modelled rock mass cohesion determined assuming a Mohr–Coulomb criterion (linear best fit) for a normal stress range of [0, 4 MPa]

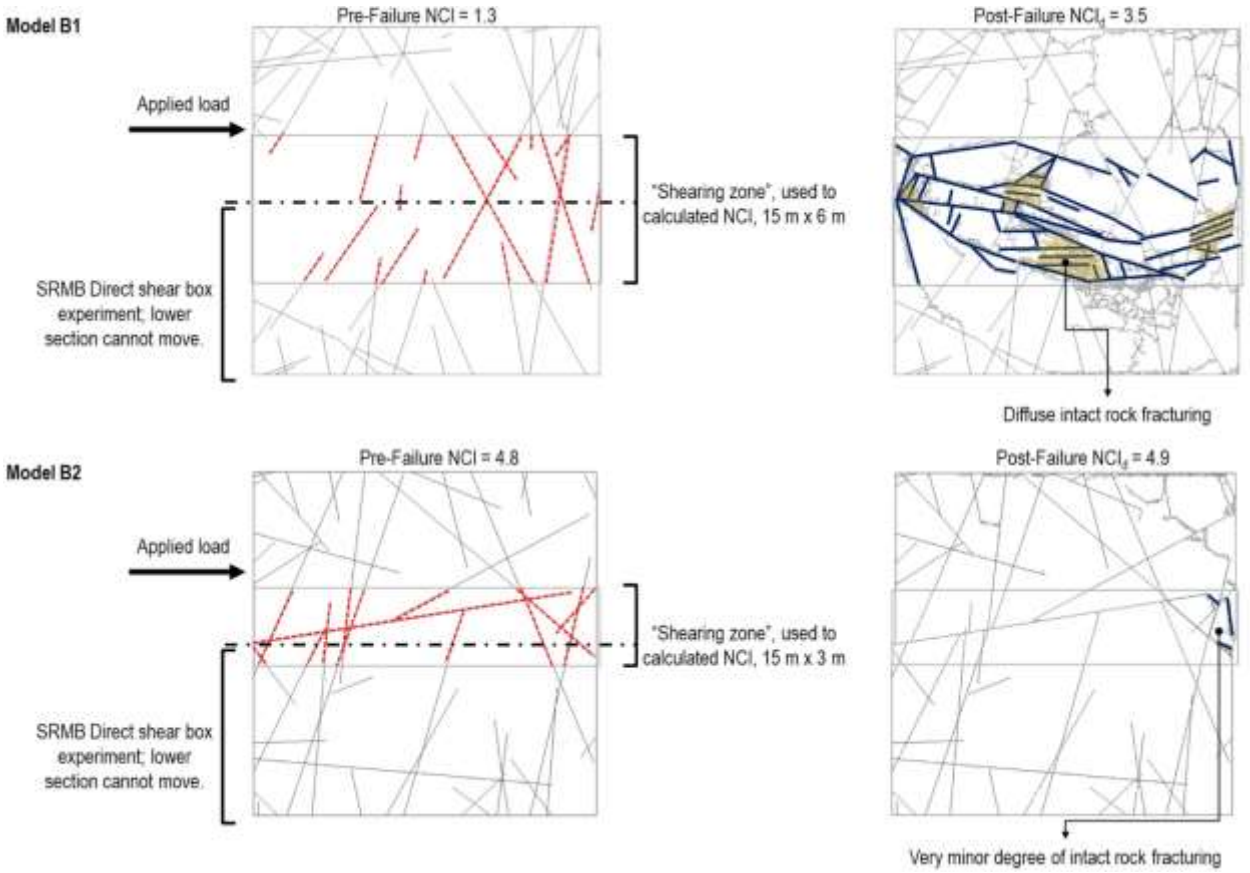


Fig. 15 Analysis of results for Models B1 and B2, pre- and post-failure

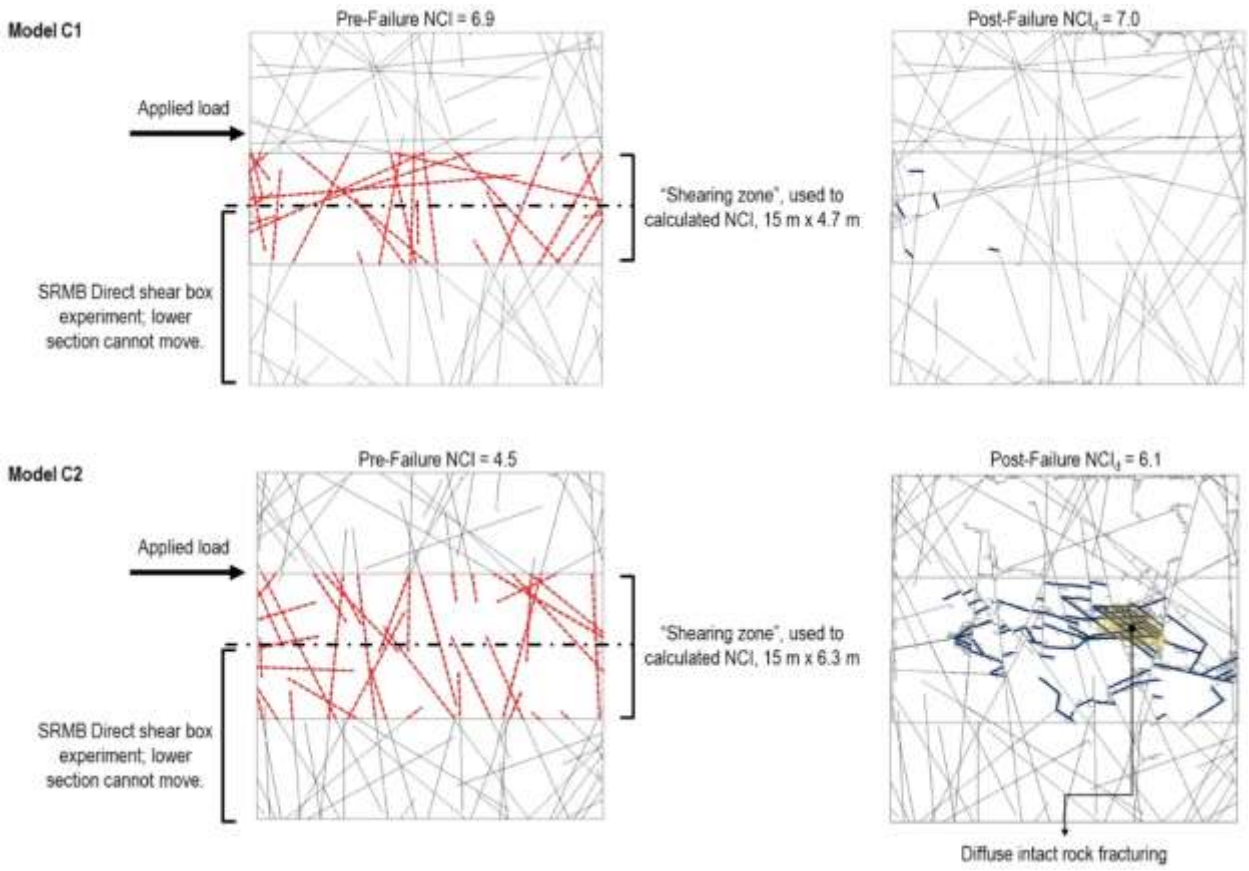


Fig. 16 Analysis of results for Models C1 and C2, pre- and post-failure

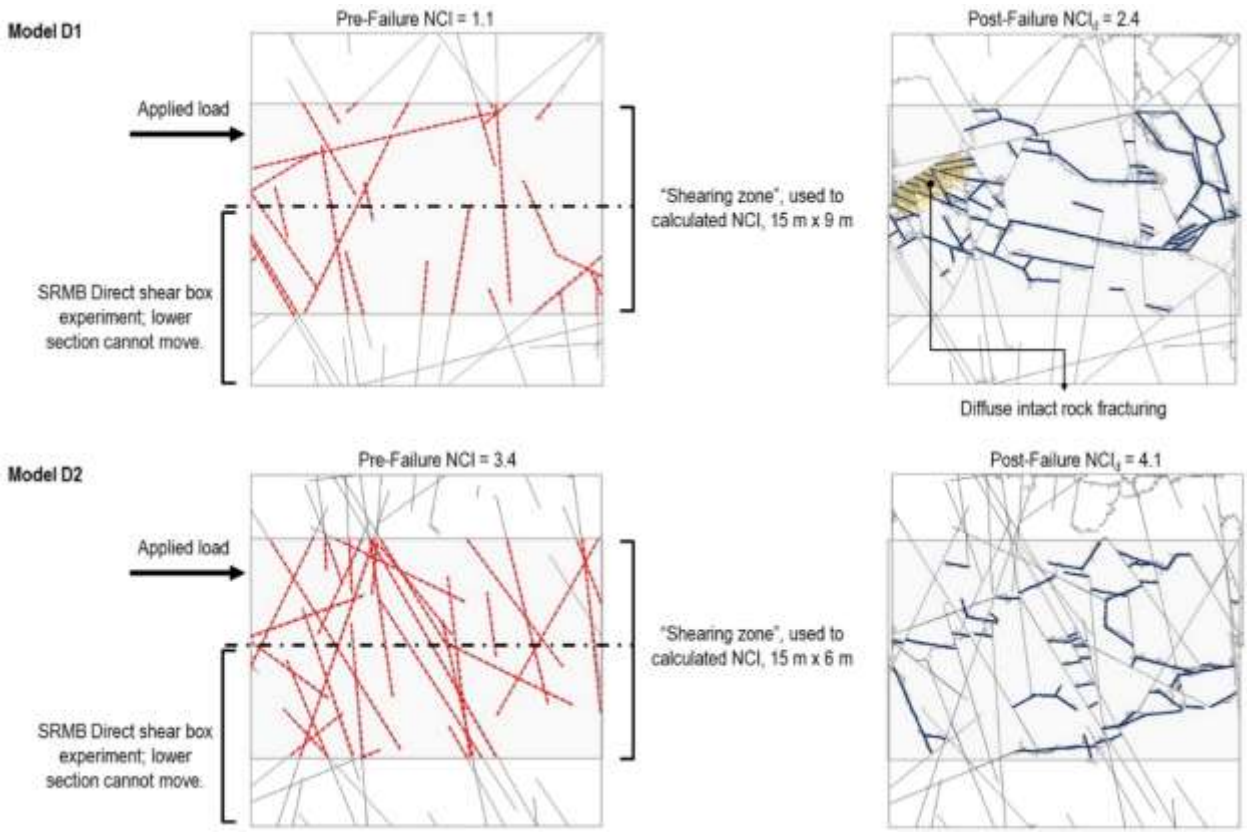


Fig. 17 Analysis of results for Models D1 and D2, pre- and post-failure

Figure 18 below shows the relationship between rock bridge potential and normalised strength for all nine SRMB models; because those models represent synthetic direct shear box experiments, the normalised strength is calculated as the ratio of modelled rock mass cohesion to intact rock cohesion. The results show that the strength of rock mass bridges could be characterized in terms of their initial and induced NCI ratings. For equivalent initial NCI rating and intact rock strength values, the different SRMB models may yield a different equivalent strength and failure paths depending on the imposed loading conditions and the variability of the natural fracture network.

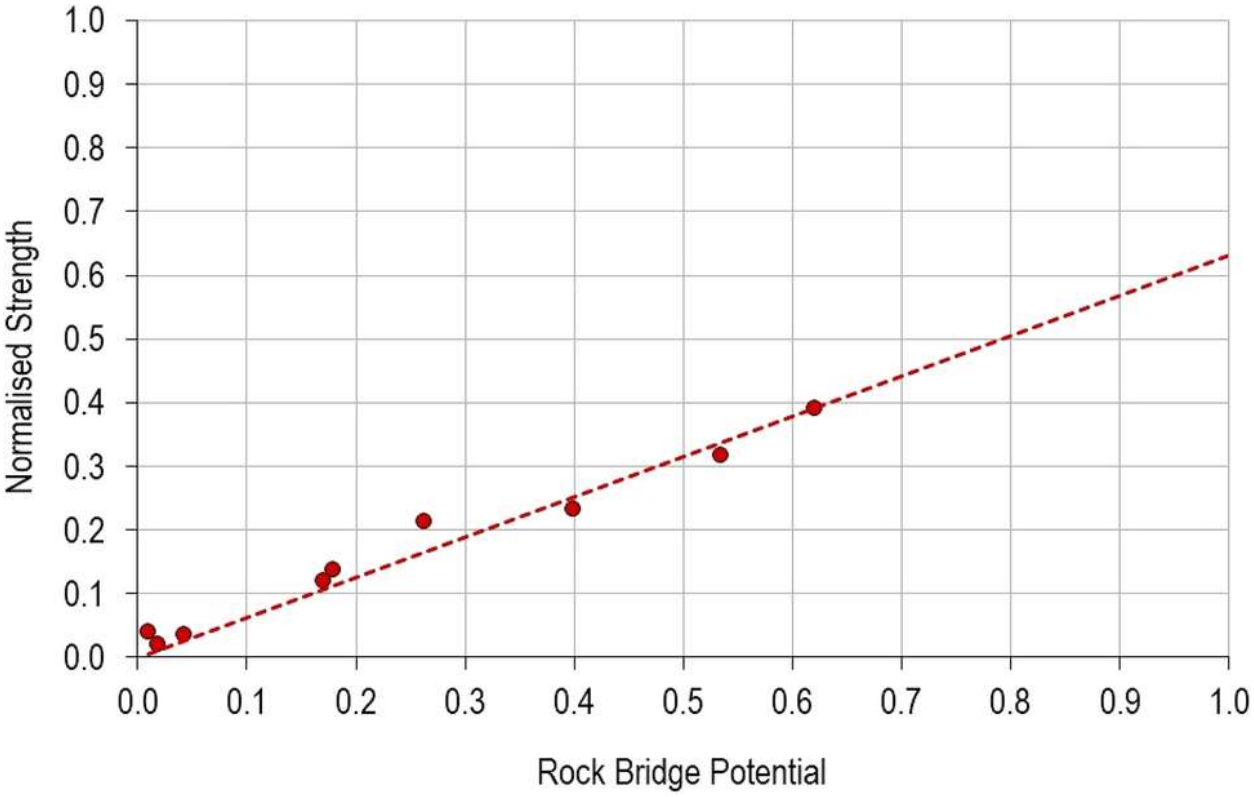


Fig. 18 Normalised strength as a function of the calculated rock bridge potential. Results for the nine SRMB models included in Table 2

The results presented in Fig. 18 suggest that the normalised strength determined for a rock bridge potential of 1 would correspond to approximately 62% of the intact rock cohesion value (i.e., 6.9 MPa). This can be explained in terms of scale effects and a reduction in rock strength with increasing sample size. Using a similar synthetic FDEM approach, Elmo et al. (2016) previously demonstrated that the strength of SRMB models at different scales decrease as the scale of the model size is increased. The same authors suggested that the reduction in strength for SRMB models up to 2-m scale (with no embedded DFN model) would follow a relationship like that proposed by Hoek and Brown (1980) for rock samples under compression. Under these assumptions, we would expect a reduction of intact rock cohesion from 11 MPa (intact rock sample) to approximately 7.2–5.9 MPa (1–2 m synthetic rock mass sample). The results presented in Fig. 18 would, therefore, suggest that even in the absence of an embedded DFN, the strength of the SRMB models would approach that of a unit cube of the rock mass.

The concept of rock bridge potential also addresses a fundamental assumption that is made in engineering design scenarios when using Jennings (1970) approach, that is the rock bridge percentage, and the resulting equivalent cohesive strength is independent of the number of

rock bridges being considered. Using the slope example shown in Fig. 19, the rock bridge coefficient (using the definition by Jennings 1970) would be the same for the two Scenarios (a) and (b). However, when considering their rock bridge potential, the NCI pre-failure for case (a) is 2/3 of the NCI pre-failure for case (b) due to the different number of fracture segments forming the hypothetical failure plane. The two scenarios would have the same NCIrb (assuming failure occurs by simply connecting the existing fracture segments). Despite Scenario (a) including two separate rock bridges and Scenario (b) including a single rock bridge, the number of intersections (I20) used in the calculation of NCIrb would be 4 and 2 for Scenario (a) and (b), respectively, thus the resulting NCIrb would be the same. Because of their different pre-failure NCI values, scenario (a) would result in a lower rock bridge potential compared to scenario (b).

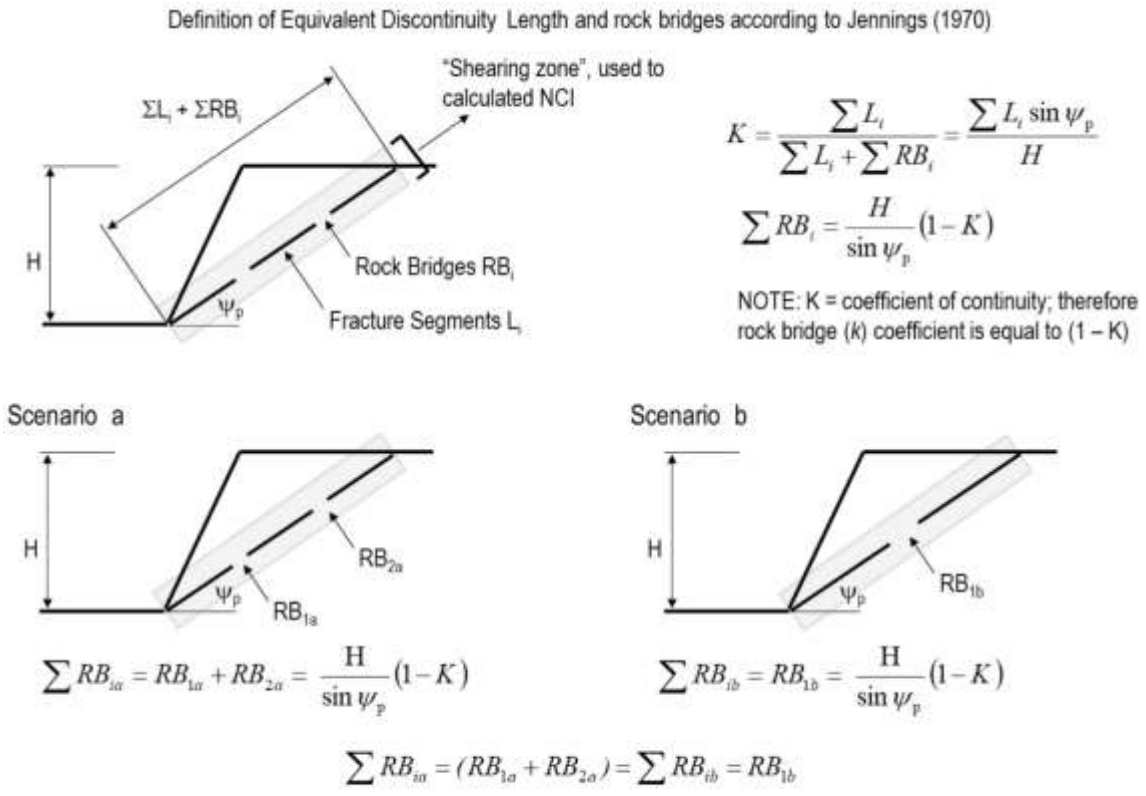


Fig. 19 Simple slope example to show how the concept of rock bridge potential can address cases in which equivalent rock bridge lengths may, erroneously, lead to consider equivalent rock mass responses

### 5.1.2 Discussion on NCI, Rock Bridge Potential and Failure Mechanisms

The objective of the numerical simulations presented herein is not to determine precise material properties, but to demonstrate the governing failure mechanisms and their association with the concept of rock bridges. It is recognised that in its current 2D formulation NCI is directionally dependent; however, as described in Sect. 2, rock bridges are indeed directionally dependent, their extent and strength being a function of the kinematic freedom and imposed loading conditions. At the same time, the theory proposed by Jennings (1970) is itself a 2D approach. Although the use 2D SRM models provides a conservative result compared to 3D models with embedded DFNs (due to the exaggerated out of plane continuity of the 2D fractures), it, however, allows for a better comparison with methods currently adopted in industry to characterise rock bridge strength.

Because of its definition and a full consideration of the network connectivity, the authors believe that the proposed rock bridge potential addresses the limitations discussed earlier concerning using rock bridge percentage as a measure of rock bridge strength; furthermore, both positive and negative step-path failure processes are combined in the definition of rock bridge potential.

A rock bridge potential of 0 could only be achieved in the case of a rock mass comprised of fully formed blocks whose failure would not result in any induced fracturing (pure sliding mechanisms). In Fig. 20, we have attempted to link the concepts of NCI and rock bridge potential to the expected failure mechanisms for rock masses with varying structural characteristics (e.g., massive, blocky and very blocky). Our approach is conceptually similar to the matrix proposed by Martin et al. (2001) and Kaiser (2019) to highlight the role of increasing rock mass damage for rock masses with equivalent GSI ratings subjected to increasing induced stresses. For massive conditions (NCI less than 2), failure is more likely to be controlled by brittle failure mechanisms, and overall rock mass failure would be associated with a larger degree of induced fracturing (i.e., rock bridge potential progressively greater than 0.4, Models B1 and D1). The behavior of a blocky rock mass would depend on the continuity of the natural fracture network and the degree of interlocking. The lower the continuity or the greater the interlocking, the higher the degree of induced fracturing we would observe at failure. Accordingly, we observe a transition from sliding (models A2, B2 and C1) to brittle failure dominated mechanisms (models A1 and C2). Note that these results refer to SRMB models with zero applied normal stress. For increasing applied normal stress conditions, the SRMB models yield a much larger degree of induced fracturing (e.g., Model A1 in Fig. 9. 0 and 2 MPa normal stress conditions), thus it is expected that the results would shift vertically into the transitional and brittle failure zones (rock bridge potential larger than 0.2 and 0.4, respectively).

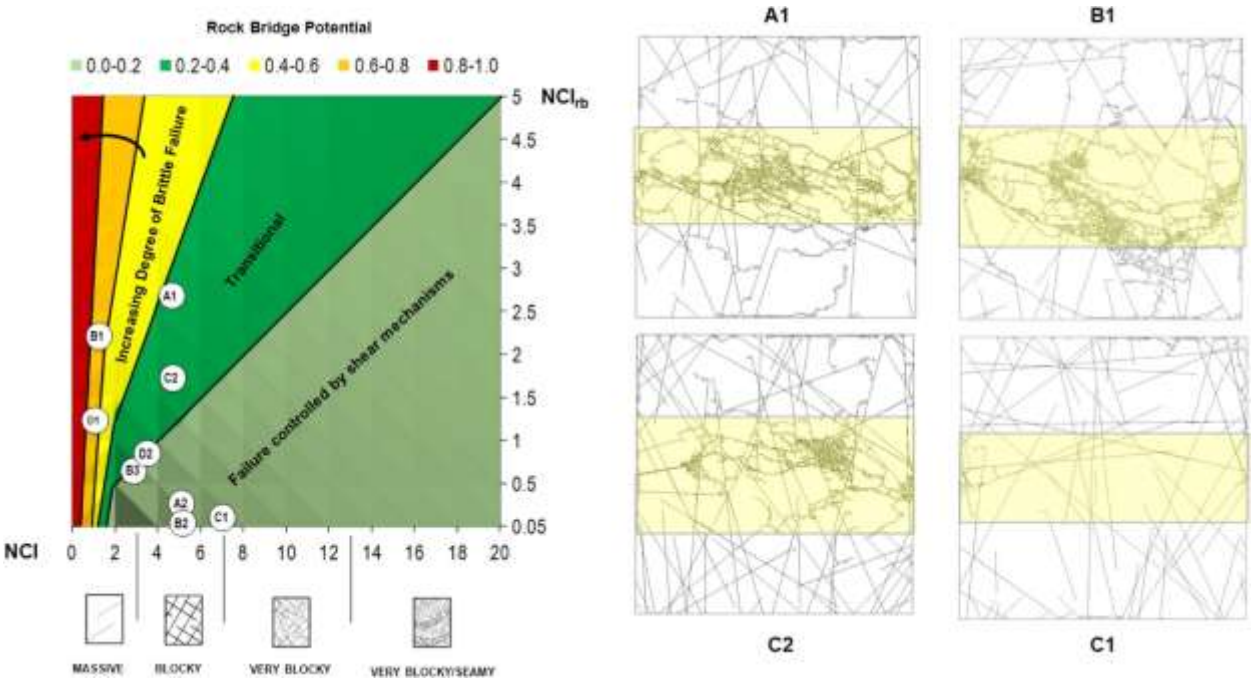


Fig. 20 Relationship between NCI, rock bridge potential and failure mechanisms for rock masses with varying structural characteristics (e.g., massive, blocky and very blocky). SRMB models with 0 MPa normal stress conditions

# 6 Conclusions

This paper has presented a series of arguments to demonstrate that the general current concept of a rock bridge, defined as the distance between existing discontinuities, is flawed, as it does not adequately consider failure mechanisms and progressive rock damage. Likewise, the validity of equations available in the literature that build on such an approach to define equivalent cohesion and friction angle parameters for an equivalent failure plane would also be in doubt, since they are limited to very specific conditions seldom encountered in the field. These issues, often ignored by engineers and practitioners, are a testimony of how revisions of established empirical methods are not so immediate (Elmo et al. 2020a, b). Rock bridges are not visible geological features; their existence is conditional to structural, stress and strength conditions, which are not necessarily constant over time.

More attention should be given to better understanding rock bridges in the context of the fracture network connectivity and damage-related processes, including time-dependent damage occurring in engineered excavations. To this purpose, the authors have presented a new rock mass quality indicator, NCI, that combines fracture length, number of fractures and number of intersections per area, while at the same time accounting for shape effects of the mapped surface area. NCI can be integrated with explicit simulations of rock damage, to

address the fundamental question of rock mass bridge strength. To date, the NCI approach has been validated using data from two different locations and four different rock mass domains. The authors are currently working to improve the NCI system based on additional case studies. Work is ongoing to develop an automated detection algorithm to provide faster measurements of NCId and rock bridge potentials using outputs from different FDEM codes.

The proposed rock bridge potential suggests that by adopting FDEM or DEM modelling techniques with fracturing capabilities over continuum modelling approaches we could gain a better understanding of rock bridge problems. Adding an explicit fracturing capability to simulations of large rock engineering problems with embedded fracture network models would inherently capture the role of rock mass damage. However, the authors acknowledge that large-scale 2D and 3D FDEM and DEM modelling is generally limited by the discrete mesh and/or particle resolution adopted in the models (Elmo and Stead 2016).

A major implication of the discussion presented in this paper is that rock bridges should be considered in terms of the risk they may pose. The emphasis should, therefore, be on considering the failure of rock bridges as hazards, while at the same time, understanding the consequence that such failure may impose. For slope problems, the hazard would be the potential for critical rock bridges related to the presence of critically oriented fractures to allow daylighting or kinematic release; non-critical rock bridges would control fragmentation and would not represent an immediate hazard. However, the degree of fragmentation due to non-critical rock bridge failure could later impact the flow/fall mechanism of the failure—i.e., rock bridges could control the size of the block involved in failure and transitions from large block failures to rockfall and rock avalanches with considerable runout. Similarly, non-critical rock bridges become a hazard when studying mass mining problems in which rock mass fragmentation is considered critical.

# References

Alghalandis YF, Elmo D (2018) Application of graph theory for robust and efficient rock bridge analysis. In: 2nd International discrete fracture network engineering conference, Seattle, WA, USA, 20–22 June 2018. Paper 733

Alghalandis YF, Dowd PA, Xu C (2015) Connectivity field: a measure for characterising fracture networks. Math Geosci 47(1):63–83

Alzo'ubi A (2009) The effect of tensile strength on the stability of rock slopes. PhD thesis, Department of Civil and Environmental Engineering, University of Alberta, Edmonton, Alberta, Canada

Arikan F, Ulusay R, Aydın N (2007) Characterisation of weathered acidic volcanic rocks and a weathering classification based on a rating system. Bull Eng Geol Environ 66(4):415–430

Baczynski NRP (2000) Stepsim4 - “Step-path” method for slope risks. In: Proc., GeoEng Int. Conf. Geotech. Geol. Eng., Melbourne, p 6

Baczynski NRP (2008) STEPSIM4 revised: network analysis methodology for critical paths in rock mass slopes. In: Proceedings of the 2008 southern hemisphere international rock mechanics symposium, September 16–19, Perth, pp 405–418

Call RD, Nicholas DE (1978) Prediction of step path failure geometry for slope stability analysis. In: Proc. of the 19th US symposium on rock mechanics, Stateline, Nevada; Int J Rock Mech Min Sci Geomech. Abst, vol 16, p 8

Dershowitz WS, Finnila A, Rogers S, Hamdi P, Moffitt KM (2017) Step path rock bridge percentage for analysis of slope stability. In: Proc. of 51st U.S. rock mechanics/geomechanics symposium, San Francisco, CA, USA. Paper 1045

Einstein HH, Veneziano D, Baecher GB, O’Reilly KJ (1983) The effect of discontinuity persistence on rock slope stability. Int J Rock Mech Min Sci Geomech 20:227–236

Elmo D (2006) Evaluation of a hybrid FEM/DEM approach for determination of rock mass strength using a combination of discontinuity mapping and fracture mechanics modelling, with emphasis on modelling of jointed pillars. Ph.D. thesis, Camborne School of Mines, University of Exeter, UK

Elmo D, Stead D (2010) An integrated numerical modelling - discrete fracture network approach applied to the characterisation of rock mass strength of naturally fractured pillars. Rock Mech Rock Eng 43(1):3–19

Elmo D, Rogers S, Stead D, Eberhardt, E (2014) A Discrete fracture network approach to characterise rock mass fragmentation and implications for geomechanical upscaling. Min Technol J 123(3):149–161

Elmo D, Stead D (2016) Applications of fracture mechanics to rock slopes. Invited chapter, rock mechanics and engineering volume 3: analysis, modeling & design, chapter 23, p 34

Elmo D, Stead D (2020) Disrupting rock engineering concepts: is there such a thing as a rock mass digital twin and are machines capable of “learning” rock mechanics. In: Int. symposium on open pit mining and civil engineering, Perth

Elmo D, Moffitt K, D’Ambra S, Stead D (2009) A quantitative characterisation of brittle rock fracture mechanisms in rock slope failures. In: Proceedings of: int. symposium on rock slope stability in open pit mining and civil engineering, Santiago, Chile

Elmo D, Moffitt K, Carvalho J (2016) Synthetic rock mass modelling: experience gained, and lessons learned. In: 50th U.S. rock mechanics symposium, Houston, TX, June 2016. Paper 777

Elmo D, Donati D, Stead D (2018) Challenges in the characterisation of rock bridges. Eng Geol 245:81–96

Elmo D, Stead D, Yang B (2020a) Disrupting the concept of rock bridges. In: Proc. 52nd int. symposium on rock mechanics, Golden, CO, June 2020. Paper 2063

Elmo D, Yang B, Stead D, Rogers S (2020b) A new discrete fracture network approach to rock mass classification. In: Proceedings of the 16th international conference on computer methods and advances in geomechanics, Turin, Italy, July 2020

Guerin A, Jaboyedoff M, Collins BD (2019) Detection of rock bridges by infrared thermal imaging and modeling. Sci Rep 9:13138. https://doi.org/10.1038/s41598-019-49336-1

Hencher SR, Lee SG, Carter TG, Richards LR (2012) Sheet joints: characterisation, shear strength and engineering. Rock Mech Rock Eng 44:1–22

Hoek E, Brown ET (1980) Underground excavations in rock. Institution of mining and metallurgy, London, p 527

Hoek E, Kaiser PK, Bawden WF (1995) Support of underground excavations in hard rock. Balkema, Rotterdam

ISRM (1981) International society of rock mechanics suggested methods for rock characterisation testing and monitoring. Brown ET (ed) Imprint Oxford, Pergamon, p 211

Jennings JE (1970) A mathematical theory for the calculation of the stability of slopes in open cast mines. In: Van Rensburg (ed) Planning open pit mines, Proceedings, Johannesburg. A.A. Balkema, Cape Town, pp 87–102

Kaiser P (2019) 8th Mueller lecture presented at the 14th ISRM Congress, Brazil, CRC Press, pp 141–182

Kemeny J (2005) Time-dependent drift degradation due to the progressive failure of rock bridges along discontinuities. Int J Rock Mech Min Sci 42(1):35–45

Martin CD, Christiansson R, Soederhaell J (2001) Rock stability considerations for siting and constructing a KBS-3 repository, SKB technical report TR-01-38. https://inis.iaea.org/collection/NCLCollectionStore/_Public/33/004/33004840.pdf?r=1

Munjiza A, Owen DRJ, Bicanic N (1995) A combined finite-discrete element method in transient dynamics of fracturing solids. Eng Comput 12:145–174

Owen DRJ, Feng YT, de Souza Neto EA, Cottrell MG, Wang F, Andrade Pires FM, Yu J (2004) The modeling of multifracturing solids and particulate media. Int J Numer Methods Eng 60(1):317–339

Pierce M, Cundall P, Potyondy P, Mas Ivars D (2007) A synthetic rock mass model for jointed rock. In: Proc. 1st Canada-US rock mechanics symposium. Vancouver, vol 1, pp 341–349

Read JR, Lye GN (1984) Pit slope design methods: Bougainville copper open cut. In: Proceedings, 5th international congress on rock mechanics, Melbourne, pp C93–C98

Rockfield (2019) Rockfield Software Ltd. Swansea. UK. Elfen version 5.7.1. http://www.rockfield.co.uk

Romer C, Ferentinou M (2019) Numerical investigations of rock bridge effect on open pit slope stability. J Rock Mech Geotech Eng 11(6):1184–1200

Sampaleanu C (2017) The role of intact rock fracture in rockfall initiation. M.Sc. thesis, Simon Fraser University, Vancouver, Canada

Sampaleanu C, Stead D, Schlotfeldt P (2017) Evaluating rockfall hazard on Stawamus Chief, Squamish, British Columbia. In: Proc. CGS Conf., GeoOttawa, p 8

Schellenberg S (2016) Phenomenal evidence and factive evidence. Philos Stud 173:875–896

Shang J, Hencher SR, West LJ, Handley K (2017) Forensic excavation of rock masses: a technique to investigate discontinuity persistence. Rock Mech Rock Eng 50:2911–2928

Spreafico M, Franci F, Bitelli G, Borgatti L, Ghirotti M (2017) Intact rock bridge breakage and rock mass fragmentation upon failure: quantification using remote sensing techniques. Photogramm Rec 32(160):513–536

Stacey P, Read J (2009) Guidelines for open pit slope design, 1st edn. CRC Press

Terzaghi K (1962) Stability of steep slopes on hard unweathered rock. Géotechnique 12:251–270

Wang R, Elmo D, Stead D, Rogers S (2017) Characterisation of rock mass representative elementary volume using RQD and a discrete fracture network approach. In: Proceedings of the 51st int. symp. rock mech., San Francisco, U.S. June 2017. Paper 760

Xu C, Dowd PA, Fowell RJ (2006) A connectivity index for discrete fracture networks. Math Geol 38(5):611–634

# Acknowledgements

A shorter version of this paper was originally prepared for presentation at the 54th US Rock Mechanics/Geomechanics Symposium (Golden, Colorado, USA, 28 June–1 July 2020) and it was later selected for publication in a special issue of Rock Mechanics and Rock Engineering. In accordance with the editor's requests, the original manuscript has been extensively revised and significantly extended before consideration by Rock Mechanics and Rock Engineering.